Stable lariats bearing a snoRNA (slb-snoRNA) in eukaryotic cells: A level of regulation for guide RNAs

Gaëlle J. S. Talross[a,1,2], Svetlana Deryusheva[a,1], and Joseph G. Gall[a,3]

[a]Department of Embryology, Carnegie Institution for Science, Baltimore, MD 21218

Contributed by Joseph G. Gall, September 10, 2021 (sent for review August 12, 2021; reviewed by Brenda L. Bass and Anita K. Hopper)

Small nucleolar (sno)RNAs guide posttranscriptional modifications essential for the biogenesis and function of their target. The majority of snoRNAs in higher eukaryotes are encoded within introns. They are first released from nascent transcripts in the form of a lariat and rapidly targeted by the debranching enzyme and nuclear exonucleases for linearization and further trimming. In this study, we report that some snoRNAs are encoded within unusually stable intronic RNAs. These intronic sequences can escape the debranching enzyme and accumulate as lariats. Stable lariats bearing a snoRNA, or slb-snoRNA, are associated with snoRNA binding proteins but do not guide posttranscriptional modification. While most slb-snoRNAs accumulate in the nucleus, some can be exported to the cytoplasm. We find that this export competes with snoRNA maturation. Slb-snoRNAs provide a previously unknown layer of regulation to snoRNA and snoRNA binding proteins.

stable lariat | snoRNA | RNA modification | guide activity

Small nucleolar RNAs (snoRNAs) represent a class of very abundant nuclear RNAs. The majority of snoRNAs guide site-specific uridine isomerization (H/ACA box snoRNAs) and 2′-*O*-methylation (C/D box snoRNAs) of ribosomal RNA (rRNA), small nuclear RNA (snRNA), transfer RNA (tRNA), and potentially other RNAs (1, 2). In vertebrates, nearly all snoRNAs are encoded within introns. snoRNAs are released in the form of a lariat and must be linearized by the debranching enzyme, DBR1, before further trimming by nuclear nucleases to their mature size, ∼60 to 300 nt. Additionally, lariats may be linearized by nuclear endonucleases, such as RNT1 in yeast, to promote maturation (3–6).

In a recent study, we analyzed RNA extracted from oocyte nuclei or germinal vesicles (GVs) of the frog *Xenopus tropicalis*. This analysis allowed us to catalog more than 400 snoRNAs in this species (7). When we examined intronic reads in the Integrative Genomics Viewer (IGV) browser, we noticed that many *Xenopus* snoRNAs overlapped with other noncoding(nc) RNAs, namely stable intronic sequence (sis)RNA.

sisRNA refers to a class of intron-derived RNA first described by our laboratory (8). sisRNAs persist for hours in cultured cell lines or even for days in the frog oocyte (8, 9). In many species, including frogs, human, mouse, and chicken, most abundant sisRNAs exist in the form of lariats (10). Unlike "canonical" intronic RNAs, sisRNAs escape linearization by DBR1 and degradation by nucleases. These lariats are unusually stable, partially due to their noncanonical C-branchpoint (10), a poor substrate for DBR1, which is most efficient on A-branched RNA (11). Additionally, lariats can be exported to the cytoplasm, a cellular compartment largely depleted of DBR1 (10).

A few reports suggest that stable nuclear lariats play a role in transcription regulation *in cis* or *in trans*; these sisRNAs tend to accumulate at the site of transcription (9, 12–14). Alternatively, circular sisRNAs can be recruited to nuclear bodies and sequester proteins, such as Dicer (15). Viral sisRNAs can also regulate host proteins presumably by sequestration (16, 17). The functions of cytoplasmic sisRNAs remains unknown.

In this study, we report that hundreds of snoRNA-encoding introns give rise to circular sisRNAs in different vertebrates. We refer to this class of sisRNAs as stable lariats bearing a snoRNA, or slb-snoRNAs. The slb-snoRNAs do not function as modification guide RNAs, yet they are associated with canonical modification snoRNP proteins (e.g., the snoRNA binding protein pseudouridine synthase dyskerin). A fraction of slb-snoRNAs can be exported to the cytoplasm, which prevents snoRNA maturation and accumulation in the nucleus. We discuss the regulatory roles that slb-snoRNAs may play in snoRNA biogenesis and in sequestration of snoRNA binding proteins.

Results

Detection of slb-snoRNAs. In a previous study, we took advantage of the GV transcriptome to annotate nearly all snoRNAs encoded in the *X. tropicalis* genome (7). As we inspected the sequence alignment of the GV transcriptome in the IGV browser, searching for snoRNA reads (Fig. 1*A*), we noticed reads that covered nearly the entire length of some snoRNA-encoding introns (306 of all 405 intronic snoRNAs) (Dataset S1). In each case, no reads were mapped to exon–intron

Significance

Small nucleolar (sno)RNAs generally guide ribosomal RNA and small nuclear RNA modifications, essential events for ribosome and spliceosome biogenesis and function. Most are processed in the nucleus from lariat intronic RNAs, which are unstable byproducts of splicing. We report here that some snoRNAs are encoded within unusually stable lariats. These stable lariats bearing a snoRNA (or slb-snoRNAs) can be found in the nucleus and cytoplasm associated with snoRNA binding proteins. They do not function as modification guide RNAs and their export competes with snoRNA maturation. Therefore, slb-snoRNAs provide a new level of regulation of snoRNAs and snoRNA binding proteins.

Author contributions: G.J.S.T., S.D., and J.G.G. designed research; G.J.S.T. and S.D. performed research; G.J.S.T. and S.D. contributed new reagents/analytic tools; G.J.S.T., S.D., and J.G.G. analyzed data; and G.J.S.T., S.D., and J.G.G. wrote the paper.

Reviewers: B.L.B., University of Utah School of Medicine; and A.K.H., The Ohio State University.

The authors declare no competing interest.

This open access article is distributed under Creative Commons Attribution-NonCommercial-NoDerivatives License 4.0 (CC BY-NC-ND).

[1]G.J.S.T. and S.D. contributed equally to this work.

[2]Present address: Department of Molecular, Cellular and Developmental Biology, Yale University, New Haven, CT 06520.

[3]To whom correspondence may be addressed. Email: gall@carnegiescience.edu.

This article contains supporting information online at http://www.pnas.org/lookup/suppl/doi:10.1073/pnas.2114156118/-/DCSupplemental.

Published November 1, 2021.

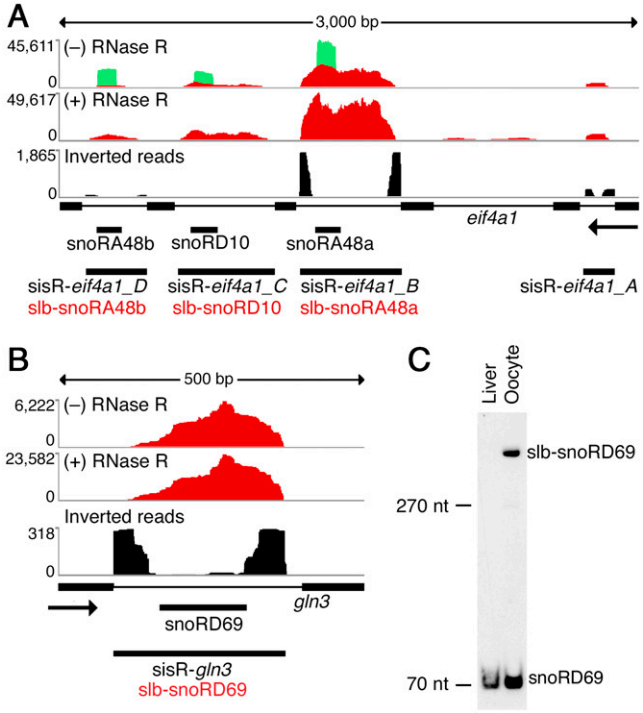

Fig. 1. Typical slb-snoRNAs in frog oocytes. (*A*) IGV browser view of the *X. tropicalis eif4a1* locus. In the nucleus, mature snoRA48 and snoRD10 (green) and slb-snoRA48 and slb-snoRD10 (red) are detected. After RNase R treatment, only slb-snoRNAs are detected. The bottom track shows "inverted" reads, indicating that the RNA is circular. (*B*) IGV browser view of the *X. tropicalis gln3* locus. Slb-snoRD69 (red) is readily detected in control and RNase R-treated samples. The bottom track shows inverted reads. (*C*) Northern blot analysis of snoRD69 in *X. tropicalis* liver (5 μg) and oocyte RNA (500 GVs) samples. Two bands were detected in RNA from oocytes: fully processed snoRD69 (lower band) and slb-snoRD69 (higher band). Note that the higher band migrates much slower than expected for the corresponding full length linear intronic RNA.

junctions. In fact, the coverage of these reads started near the 5′ splice site and ended a little upstream of the 3′ splice site (Fig. 1*A*, red coverage). This pattern suggests that the oocyte accumulates stable partially processed intronic snoRNAs in the nucleus.

Because most abundant sisRNAs accumulate as lariats (18), we wondered whether these partially processed snoRNAs also accumulated as lariats. We analyzed a dataset of the circular transcriptome that we generated by treating nuclear RNA with RNase R, a 3′-5′ exonuclease that degrades linear RNA and leaves circular RNA intact (18). As expected, we could no longer detect mature linear snoRNAs in this dataset. However, we detected reads that mapped throughout the intron, which is consistent with the detection of a circular intronic RNA (Fig. 1*A*, red coverage). Additionally, we detected numerous reads that could map to the linear genome only when they were segmented and rearranged (*SI Appendix*, Fig. S1*A*). These so called "inverted" reads correspond to the junctions of the circular RNA (Fig. 1*A*, black coverage). Thus, these data demonstrated that a fraction of some snoRNAs can be stabilized in the form of a lariat.

To confirm the existence of stable lariats encoding snoRNAs, we analyzed *X. tropicalis* GV RNA by Northern blotting. Using a probe specific for snoRD69 (Fig. 1*B*), we detected a band of about 70 nt in length, corresponding to the mature form, in liver and oocyte RNA. A higher band was readily detected only in the oocyte RNA lane (Fig. 1*C*). This higher molecular-weight band ran slower than the expected linear intronic RNA, consistent with it being a circular molecule. We observed a similar pattern when we used a probe against the mature snoRA48, although the lariat was detected at a lower level than the mature snoRNA (*SI Appendix*, Fig. S2*A*). We conclude that, in frog oocytes, a fraction of certain snoRNAs can accumulate in a lariat form in addition to the mature linear form. We refer to these circular transcripts as stable lariats bearing a snoRNA or slb-snoRNAs.

Slb-snoRNAs tend to be more abundant than other nuclear circular sisRNAs (*SI Appendix*, Fig. S3). Nevertheless, some abundant lariats did not encode a known snoRNA. This observation poses the question whether these abundant sisRNAs show similarities with slb-snoRNAs. SnoRNAs form a stable stereotypical structure and contain essential short sequences known as "boxes": C/C′ (RUGAUGA) and D/D′ (CUGA) in box C/D snoRNAs, or H (ANANNA) and ACA (AYA) in box H/ACA snoRNAs. We searched for such motifs within the sequence of the abundant circular sisRNAs (fragments per kilobase of transcript per million mapped reads [FPKM] ≥ 100 in an RNase R experiment, ∼1,300 introns) using the prediction software snoReport 2.0 (19). We found snoRNA motifs (score ≥ 0.9) within 75 sisRNAs, which included 33 of the 63 known snoRNAs that overlap with abundant lariats. Altogether, 8% (105) of abundant lariats contain snoRNAs or snoRNA motifs (Dataset S1). About 90% of these abundant lariats were shorter than 500 nt. Therefore, we surveyed annotated introns that were 100- to 500-nt long and did not code for a stable lariat (∼7,500 introns); only ∼2% of these introns contained snoRNA motifs. Altogether, we showed that the frog oocyte accumulates hundreds of stable lariats bearing a snoRNA or a snoRNA-like sequence. Furthermore, there is some enrichment of snoRNA motifs in stable lariats compared to unstable lariats of the same size.

Are slb-snoRNAs limited to the *Xenopus* oocyte? Previously, we carried out an RNA high-throughput sequencing study of circular RNA purified from cells treated with α-amanitin, a transcription inhibitor, and identified hundreds of stable lariats in human, mouse, chicken, and frog cell lines. This analysis led to the annotation of hundreds of sisRNAs (10). We reexamined these sisRNAs and found that 8 encoded a snoRNA in human HeLa cells, 6 in mouse 3T3 cells, 3 in chicken DF1 cells, and 11 in frog *Xenopus laevis* XTC cells. There was little overlap across snoRNA orthologs (Fig. 2*A* and Dataset S1). Additionally, across all four analyzed species, the snoReport 2.0 algorithm predicted a snoRNA motif in 391 sisRNAs. Of the 391, 24 corresponded to the annotated snoRNAs mentioned above, and 188 showed high predictability scores (≥0.9), including 14 that had a perfect score (=1) (Fig. 2*B* and Dataset S1).

There are three lines of evidence for the circular nature of these slb-snoRNAs drawn from our previously generated RNA-sequencing (RNA-seq) data for RNase R-treated samples (10). First, we observed that sisRNAs bearing a snoRNA persisted after the RNase R treatment (Fig. 2*A*). Second, intronic reads were not restricted to the snoRNA sequence; instead, they extended from the 5′end to the branchpoint. Finally, for some snoRNA-bearing sisRNAs, we detected unconventional reads containing branchpoint regions linked to the 5′ ends of introns. These reads correspond to the junction of lariats (Fig. 2*A*, inverted reads tracks).

Importantly, we confirmed by RT-PCR that the circular snoRNA-bearing sisRNAs are indeed lariats. We generated cDNA from RNA extracted from α-amanitin–treated cells using either Episcript RT, a reverse transcriptase that is active across branchpoints, or AMV-RT, a reverse transcriptase that terminates at branchpoints (18). Intronic cDNA produced with either enzyme could be amplified using inward facing primers. However, with outward-facing primers, only cDNA generated with Episcript RT was amplified (Fig. 2*B* and *SI Appendix*, Fig.

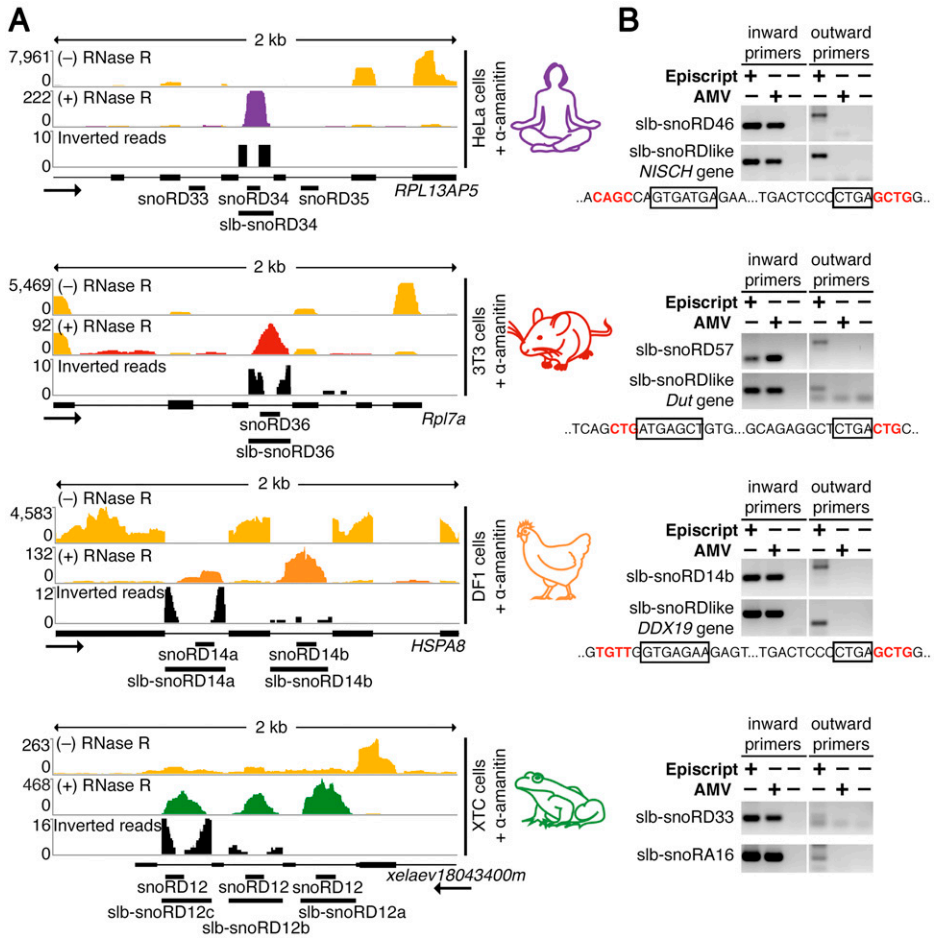

Fig. 2. Identification of slb-snoRNAs in cell lines from different vertebrate species. (*A*) IGV browser view of a typical gene encoding a circular sisRNA that overlaps with a snoRNA from human, mouse, chicken, and frog. Unlike exonic reads (yellow), intronic reads are detected in RNA samples treated with RNase R, shown in purple (human), red (mouse), orange (chicken), and green (frog). In black is the coverage of intronic inverted reads. These unconventional reads demonstrate that the intronic transcripts are circular. (*B*) RT-PCR analysis of slb-snoRNAs in the four studied species. Reverse transcription was carried out with either Episcript-RT or AMV-RT. Intronic cDNA was amplified by PCR using inward and outward primers; the latter detect circular molecules only (see schematics in *SI Appendix*, Fig. S1*B*). Predicted snoRNA motifs for the tested slb-snoRD-like transcripts are shown below the corresponding gel images. Terminal stems (red) and predicted C and D boxes (black frames) are highlighted.

S1*B*). The specificity of the PCR products was confirmed by sequencing. Thus, we demonstrated that many snoRNAs and snoRNA-like sequences were stabilized in the form of a lariat in cell lines from various vertebrate species.

Slb-snoRNAs Do Not Function as Modification Guide RNAs. Can slb-snoRNAs guide 2′-*O*-methylation and pseudouridylation? In yeast, the *dbr1Δ* strain, which is mutant for the debranching enzyme DBR1, is viable and accumulates lariats (3). While the majority of yeast snoRNAs are expressed from independent mono or polycistronic genes, eight are encoded within introns. In *dbr1Δ,* these intronic guide RNAs cannot be processed properly, and therefore accumulate mostly in the form of a lariat and partially processed linear transcripts (4). Remarkably, even when mature snoRNA molecules are barely detectable, as in the case of snR24, positions targeted for modification by this guide RNA (C1437, C1449, and C1450 of 25S rRNA) remain properly modified (4). Although the authors of the early studies thoughtfully stated that "unprocessed intronic U24 snoRNA appears to function in 2′-*O*-methylation," it was tempting to "suggest that pre-U24 in the lariat form is functional" (4).

We first started questioning the possibility of snoRNA function in the lariat form when we could not detect modifications mediated by snoRA29 in human 18S and 28S rRNAs (7). SnoRA29 is highly conserved across vertebrate species, yet in humans it accumulates only in a partially processed form, most likely a lariat (Fig. 3*A*). Indeed, the high molecular-weight band persisted in human RNA samples after RNase R treatment, which indicates its circular nature. One could argue that human slb-snoRA29 accumulates at very low levels, which may not be sufficient for modification activity. Furthermore, the 3′ terminus of human snoRA29 sequence has a point mutation in a canonical ACA box, which may affect guide RNA functions (Fig. 3*B*).

We made various constructs to express ectopically either slb-snoRA29 or fully processed snoRA29, with or without restoration of the ACA box (Fig. 3*C*). Only fully processed snoRA29, either human with the restored ACA box or mouse as a positive control (Fig. 3*D*), could induce pseudouridylation of 28S rRNA at position 45 (Fig. 3*E*) and 18S rRNA at position 220 (*SI Appendix*, Fig. S4) in HeLa cells. Importantly, mature human snoRA29 was expressed at very low levels, yet it could mediate rRNA modification. At the same time, twofold overexpression of human slb-snoRA29, regardless of the point mutation in the ACA box (Fig. 3*D*), was not sufficient to modify 28S-45 and 18S-220 (Fig. 3*E* and *SI Appendix*, Fig. S4).

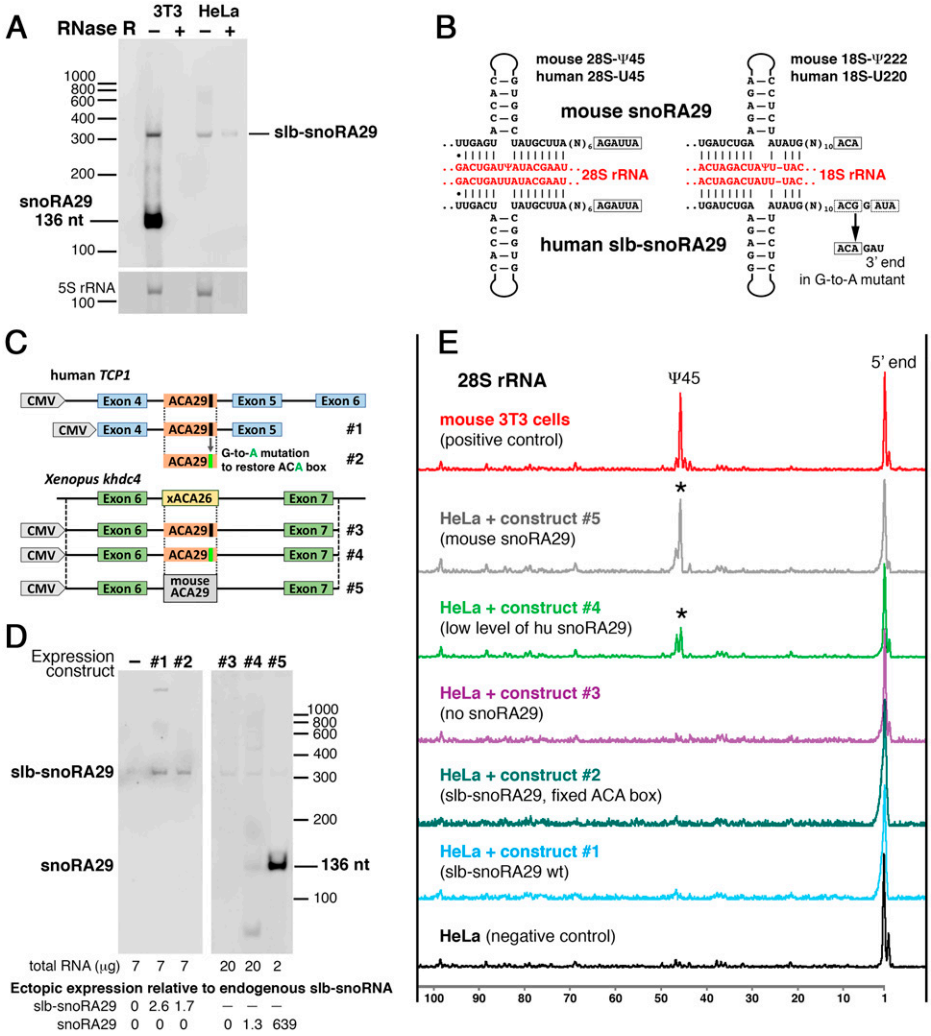

Fig. 3. Testing snoRA29 modification activities in mouse and human cells. (*A*) Northern blot analysis of snoRA29 in mouse (3T3) and human (HeLa) RNA samples treated with RNase R. Fully processed snoRA29 was detected only in control mouse RNA. In human RNA, the snoRA29 sequence is present only in the high molecular-weight band; this band is resistant to RNase R, indicating its circular nature. No snoRA29^{+} bands persist in mouse RNA treated with RNase R, indicating that in mouse both snoRA29 and the higher molecular-weight band are linear molecules; the latter represents partially processed mouse snoRA29-encoding intron. 5S rRNA served as the control for loading and RNase R treatment efficiency. (*B*) Postulated base pairing of snoRA29 with 18S and 28S rRNAs. (*C*) Diagram of constructs for ectopic snoRA29 expression in HeLa cells. (*D*) Northern blot analysis of human and mouse snoRA29 expression in HeLa cells transfected with the constructs depicted in *C*. Amount of total RNA loaded on a gel and relative expression levels of ectopic slb-snoRA29 and mature snoRA29 are indicated at the bottom. (*E*) Mapping pseudouridines in the 5′ terminal region of 28S rRNA from mouse 3T3 cells and human HeLa cells, control and transfected with 5 snoRA29 expression constructs shown in *C* and *D*. Mouse 28S rRNA is normally pseudouridylated at position 45 (top red trace). This modification is absent in human 28S (bottom black trace). Expression of fully processed snoRA29, either mouse (construct #5, gray trace) or human (construct #4, green trace), induces 28S-Ψ45 (stars) in HeLa cells. Expression of snoRA29 in the lariat form (construct #1, blue trace and construct #2, dark green trace) cannot induce pseudouridylation of U45 in human 28S rRNA. To make all traces comparable, the *y* axis was scaled for each sample relative to total arbitrary fluorescence intensity of all detected peaks in a sample, which corresponds to the amount of analyzed RNA molecules.

X. laevis snoRA75 provided another hint that slb-snoRNAs may not be functional as modification guide RNAs. We previously identified snoRA75 in two frogs of the same genus, *X. tropicalis* and *X. laevis* (7). The orthologs have almost identical structure (Fig. 4 *A* and *B*), yet mature snoRA75 is expressed in *X. tropicalis* but not in *X. laevis* (Fig. 4 *C* and *D*). Accordingly, *X. laevis* 18S rRNA lacks pseudouridylation of U93 (Fig. 4*E*). In oocytes, we detected snoRA75 expression in both *X. tropicalis* and *X. laevis* by RNA-seq and Northern blotting. However, *X. laevis* snoRA75 is expressed only in the form of a lariat (Fig. 4 *C* and *D*). Although slb-snoRA75 is very abundant and concentrates in GVs, where RNA modification normally occurs, 18S-U93 is not modified in *X. laevis* oocytes either (Fig. 4*E*). These results suggest that slb-snoRNAs and slb-snoRNA–like RNAs do not support posttranscriptional modifications.

To further explore the modification activity of snoRNAs in the form of lariats, we returned to the yeast cell system. Since the partial processing of snoRNAs in the *dbr1Δ* mutant strain could be driven by RNT1, an endonuclease involved in snoRNA processing (6), we naively expected to distinguish lariat and partially processed snoRNA activities using a double mutant, *dbr1Δrnt1Δ*. However, in the *dbr1Δrnt1Δ* mutant strain, all eight intronic snoRNAs still accumulated in the lariat, partially processed, and mature forms, although the latter two are at low levels (*SI Appendix*, Fig. S5*A*), and normal rRNA modification patterns were detected (*SI Appendix*, Fig. S5*B*). Notably, independently transcribed snoRNAs were barely detectable in *dbr1Δrnt1Δ* (*SI Appendix*, Fig. S5*C*), yet we still detected modifications at their target positions (*SI Appendix*, Fig. S5*B*). It appears that yeast endogenous snoRNA processing machinery

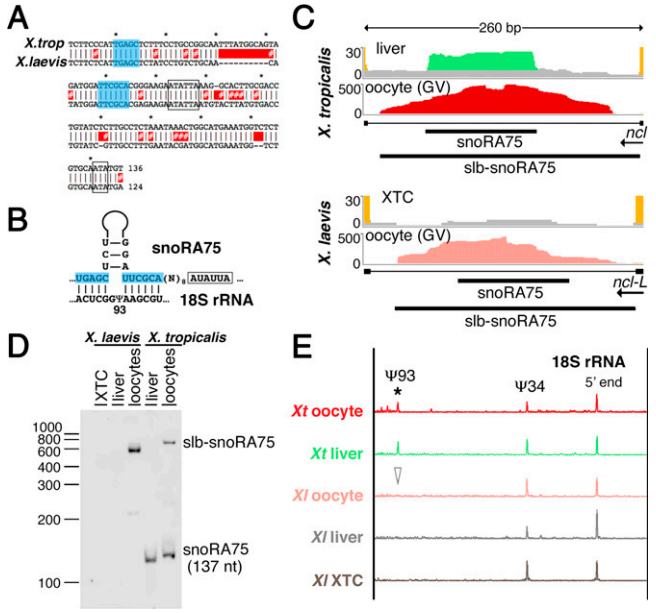

Fig. 4. *X. tropicalis* and *X. laevis* snoRA75 and slb-snoRA75. (*A*) Alignment of the two snoRA75 orthologs. The antisense element for positioning 18S-Ψ93 is highlighted with blue; the H and ACA boxes are framed with black lines. (*B*) Postulated base-pairing between snoRA75 and 18S rRNA. (*C*) IGV browser view of snoRA75 and slb-snoRA75 in oocyte and somatic tissues of *X. tropicalis* and *X. laevis*. (*D*) Northern blot analysis of snoRA75 in somatic cells, the XTC cell line and liver (10 μg of total RNA per lane) and oocytes (300 GVs) from *X. laevis*, and in liver (7 μg of total RNA) and oocytes (100 GVs) from *X. tropicalis*. Fully processed snoRA75 was detected only in *X. tropicalis* liver and oocyte RNA samples. High molecular-weight bands were detected in oocytes from both frogs; these bands migrate much slower than expected for linear full-length intronic RNA molecules, which is characteristic of intron lariats. (*E*) Mapping pseudouridines in the 5′ terminal region of *Xenopus* 18S rRNA. *X. tropicalis* 18S rRNA from liver (green trace) and oocytes (red trace) is pseudouridylated at positions 34 and 93 (star). *X. laevis* 18S rRNA is modified at position 34 but not at position 93 (arrowhead) in any tissues, including oocytes (pink trace), liver (gray trace), and the cultured cell line XTC (bottom brown trace). Traces are scaled as in Fig. 3*E*.

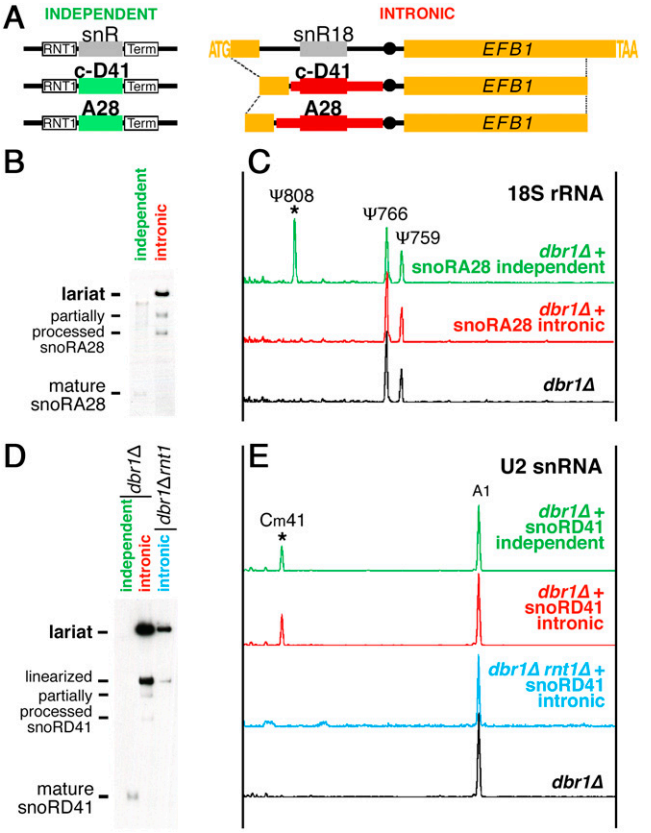

Fig. 5. Testing slb-snoRNA modification guide activities in the yeast cell system. (*A*) Schematic of DNA constructs made for expression in yeast of fully processed linear snoRNAs (independent) and snoRNAs in the form of lariats (intronic). A28 is *X. tropicalis* snoRA28; c-D41 is chimeric snoRD41 with antisense element for U2-C41 instead of 28S-U4276 (yeast 25S-U2729). RNT1 cleavage site and snR13 terminator are depicted. Intronic constructs are made by intron replacement in the yeast *EFB1* gene. *Xenopus*-specific intronic regions are shown in red. (*B*) Northern blot analysis of *xt*snoRA28 expressed from independent and intronic constructs in yeast *dbr1Δ* strain. Mature snoRA28 is expressed only from the independent construct. Expression from the intronic construct produced snoRA28 in the lariat form, and partially processed linearized lariats. (*C*) Mapping pseudouridines in 18S rRNA from the *dbr1Δ* yeast strain. Normally, pseudouridines are detected at positions 759 and 766 in yeast 18S (bottom black trace). An additional pseudouridine is detected at position 808 (star) when fully processed *xt*snoRA28 is expressed from the independent construct (green trace), but not when *xt*snoRA28 is expressed in the lariat form from the intronic construct (red trace). (*D*) Northern blot analysis of *xt*snoRD41 expression from independent and intronic constructs in yeast *dbr1Δ* and *dbr1Δrnt1Δ* strains. Mature snoRD41 is expressed only from the independent construct. Expression from the intronic construct produced lariats and their linearized forms in both mutants (presumably broken during RNA preparation). Note that partially processed transcripts can be detected in the *dbr1Δ* single mutant in addition to the lariats. (*E*) Analysis of 2′-*O*-methylation in yeast U2 snRNA. Normally, yeast snRNAs do not have 2′-*O*-methylated residues (bottom black trace). Expression of fully processed (top green trace) or partially processed snoRD41 (red trace) induced 2′-*O*-methylation of C41 in yeast U2 snRNA (star). In the *dbr1Δrnt1Δ* double mutant, snoRD41 is expressed from the intronic construct only in the form of a lariat and cannot induce 2′-*O*-methylation of U2 snRNA (blue trace).

is very robust. It has multiple back-up mechanisms to ensure proper modification of functionally important RNA molecules.

We proposed that vertebrate slb-snoRNAs, unlike endogenous yeast intronic snoRNAs, may be resistant to alternative processing, and in the *dbr1Δ* and *dbr1Δrnt1Δ* yeast mutant strains the exogenous slb-snoRNAs will accumulate exclusively in a lariat form. We selected two relatively abundant *X. tropicalis* slb-snoRNAs: slb-snoRA28 and slb-snoRD41. Advantageously, vertebrate snoRA28 mediates pseudouridylation of 18S rRNA at a position that is not modified in yeast (18S-U808). Furthermore, we showed previously that this modification can be induced in yeast by the expression of a corresponding guide RNA (7). Unfortunately, the target position of snoRD41 is modified in yeast (25S-Um2729). To minimize alterations in the already sensitive mutant strains, we opted for the replacement of the antisense element in snoRD41 to target U2 snRNA at position C41 instead. Yeast U2-C41 is not normally modified, but this modification can be easily induced (20).

We inserted the *Xenopus* slb-snoRNAs in the yeast *EFB1* gene, in place of the intron encoding snR18, but preserved yeast canonical splicing motifs (Fig. 5*A*). As a control, we made constructs to express snoRA28 and snoRD41 as independent genes (Fig. 5*A*). When we expressed snoRA28 from the independent gene construct in the *dbr1Δ* strain, low levels of mature snoRA28 were detected by Northern blot (Fig. 5*B*) and 18S-U808 became modified in these cells (Fig. 5*C*, green trace). Similar to endogenous yeast snoRNAs, a minimal amount of fully processed snoRA28 is sufficient for modification. At the same time, when we expressed intronic snoRA28 in *dbr1Δ*, mature snoRA28 failed to accumulate. Instead, we detected slb-snoRA28 and linearized slb-snoRA28 (Fig. 5*B*). Even though the lariat and "partially processed" linearized transcripts were abundant, they could not induce pseudouridylation

of 18S-U808 (Fig. 5*C*, red trace). These results demonstrate that neither partially processed box H/ACA snoRNA nor its lariat are capable of mediating RNA modification.

Intriguingly, when we transformed the *dbr1Δ* mutant strain with the snoRD41 constructs, U2-C41 was modified by both independently transcribed and intronic chimeric guide RNAs (Fig. 5*E*, green and red traces, respectively), even though in the case of intronic construct, mature snoRD41 was not evident (Fig. 5*D*). When snoRD41 was expressed from the intronic construct, we detected slb-snoRD41 and the partially processed form of snoRD41; the guide RNA activity could come from either or both forms of this box C/D snoRNA. We next transformed the *dbr1Δrnt1Δ* double mutant. In this mutant, the intronic chimeric snoRNA accumulated mostly as a lariat (Fig. 5*D*), and U2-C41 was not modified (Fig. 5*E*, blue trace). Because the levels of slb-snoRD41 in the *dbr1Δrnt1Δ* strain were three to five times higher than the levels of linear snoRD41 expressed as an independent transcript (Fig. 5*D*), we concluded that snoRNAs in the lariat form are not functional as modification guide RNAs. Based on all these experiments, we rule out the possibility that slb-snoRNAs can guide posttranscriptional modifications.

Canonical snoRNP Core Protein Can Bind to slb-snoRNA. To function as modification guide RNAs, snoRNAs form a snoRNA–protein complex (snoRNP) with four different proteins, including one catalytic enzyme: the pseudouridine synthase dyskerin in H/ACA box snoRNPs or the methyltransferase fibrillarin in C/D box snoRNPs. Often the snoRNP assembly occurs cotranscriptionally. Since we found that snoRNAs in a lariat form could not guide posttranscriptional modifications, we wondered if canonical snoRNP proteins bind stably to slb-snoRNAs. Originally, the human snoRA29 sequence, which exists only in a lariat form (Fig. 3*A*), was identified in an RNA fraction coprecipitated with GAR1 protein, one of the four core proteins in box H/ACA snoRNPs (21). This finding indicated that snoRNP proteins can bind to slb-snoRNAs. We decided to focus on dyskerin, the only snoRNA binding protein with catalytic activity and an RNA binding domain, and to test if it is associated with slb-snoRNA. As an RNA counterpart for this assay, we selected an abundant slb-snoRNA, *Xenopus* slb-snoRA75, because this lariat could be ectopically expressed at high levels and easily detected by Northern blotting and RT-PCR.

We coinjected *X. laevis* oocytes with a DNA construct encoding HA-tagged dyskerin and a construct optimized to express stable lariats (10). The latter construct included the *X. tropicalis*

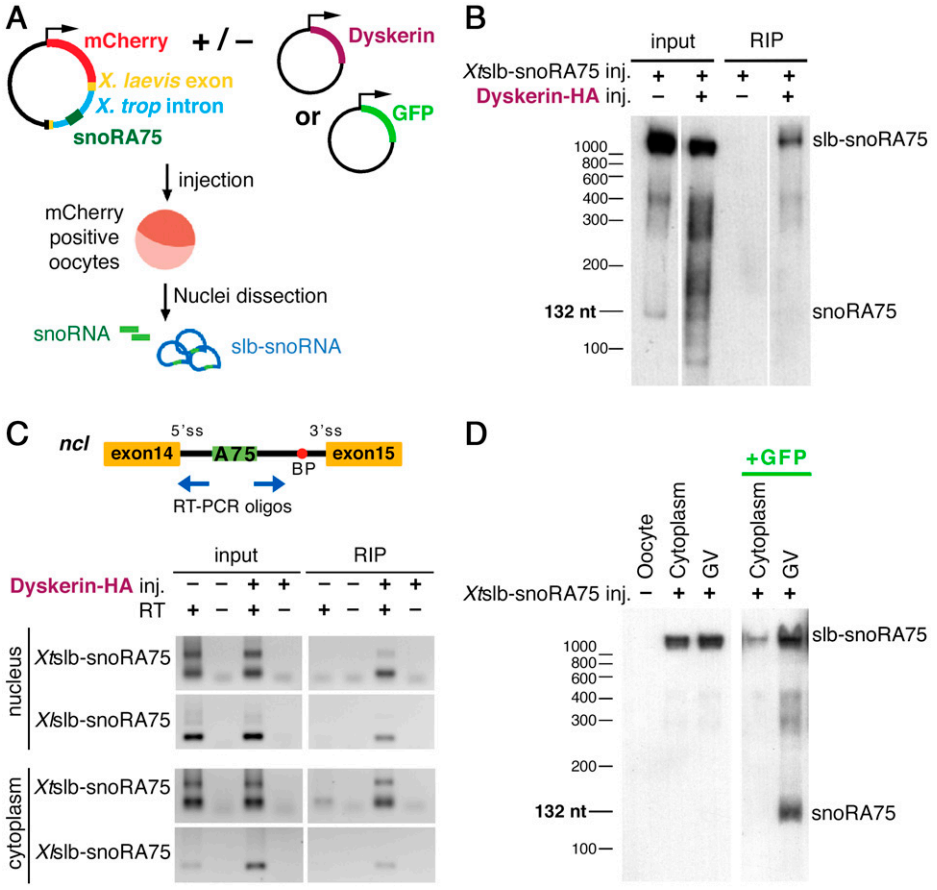

Fig. 6. Ectopic expression of slb-snoRNA, its coimmunoprecipitation with dyskerin and its active export to the cytoplasm. (*A*) Diagram of expression constructs used for ectopic expression of slb-snoRNA in *X. laevis* oocytes. (*B*) Northern blot analysis of *X. tropicalis* snoRA75 and slb-snoRA75 coprecipitated with dyskerin. Ectopic *xt*slb-snoRA75 is detected in both input samples: oocytes coinjected with HA-tagged dyskerin and mock coinjected. The *xt*slb-snoRA75 coprecipitated only in the presence of HA-tagged dyskerin. (*C*) RT-PCR analysis of RNA coimmunoprecipitated with dyskerin. Inverted primers (blue arrows in the gene model schematic) were used to detect slb-snoRNA only. Ectopically expressed *xt*slb-snoRA75 and endogenous *xl*slb-snoRA75 coprecipitated with dyskerin in both nuclear and cytoplasmic fractions. (*D*) Northern blot analysis of *xt*slb-snoRA75 accumulation in *X. laevis* oocytes coinjected with a construct for expression of GFP mRNA as a competitor. When the *xt*snoRA75 construct is injected alone, ectopic slb-snoRA75 (higher band) is detected in the nucleus and cytoplasm of *X. laevis* oocytes; expression of mature *xt*snoRA75 is detectable only in the nucleus using much longer exposures (not shown). RNA from one dissected nucleus (GV) and cytoplasm of injected oocytes was loaded per lane. After coinjection with 750 pg of GFP construct, slb-snoRA75 is detected mostly in the nucleus, and fully processed snoRA75 is accumulated in the nucleus at high levels.

(*xt*) slb-snoRA75 sequence inserted in a portion of the *X. laevis ncl* gene, downstream of mCherry (Fig. 6*A*). Two days after injection, nuclei of mCherry$^+$ oocytes were isolated, lysed, and subjected to RNA coimmunoprecipitation using an anti-HA tag antibody. Using Northern blotting, we detected ectopically expressed *xt*slb-snoRA75 in the RNA fraction coimmunoprecipitated with HA-tagged dyskerin, which indicated that dyskerin was bound to the lariat (Fig. 6*B*). We then tested whether endogenous *X. laevis* (*xl*) slb-snoRA75 interacts with dyskerin as well. We performed RT-PCR analysis using outward facing primers to detect *xl*slb-snoRA75. It is important to point out that newly synthesized endogenous RNA is virtually undetectable in this assay. Surprisingly, we found endogenous *xl*slb-snoRA75 was also coprecipitated with HA-tagged dyskerin (Fig. 6*C*). These results suggest that dyskerin forms a dynamic RNP complex with slb-snoRNAs, and that snoRNP can bind to slb-snoRNA posttranscriptionally.

slb-snoRNAs Can Be Exported to the Cytoplasm and This Export Competes with Mature snoRNA Processing. We previously reported that most abundant lariats are exported to the cytoplasm. Naturally, we questioned if slb-snoRNAs were also exported. As an initial experiment, we searched through RNA-seq datasets from RNase R-treated cytoplasmic samples. Because snoRNAs are typically found in the nucleus, we expected that slb-snoRNAs would be restricted to the nucleus. Remarkably, we detected 29 slb-snoRNAs in the cytoplasm of *X. tropicalis* oocytes (*SI Appendix*, Fig. S2*B*, blue coverage, and Dataset S1). Additionally, about 2% of the most abundant cytoplasmic sisRNAs (FPKM ≥100 in RNase R experiment, ∼2,000 introns analyzed) have high-probability snoRNA motifs. Cytoplasmic lariats did not show an enrichment for such motifs relative to unstable introns of the same size.

Typical sisRNAs are exported to the cytoplasm by the NXF1/NXT1 machinery (10). To test if slb-snoRNAs were also actively exported, we carried out the export competition assay for an slb-snoRNA. We injected *xt*slb-snoRA75 construct, separated nuclear and cytosolic RNA fractions from mCherry$^+$ oocytes, and analyzed these RNAs by Northern blotting. Both *xt*snoRA75 and *xt*slb-snoRA75 were detected in the nuclear fraction, but only *xt*slb-snoRA75 accumulated in the cytoplasm (Fig. 6 *B* and *D*). When the *xt*slb-snoRA75 construct was coinjected with large amount of the GFP expression construct, a competitor for the NXF1/NXT1 export machinery, accumulation of *xt*slb-snoRA75 in the cytoplasm was impaired, suggesting that slb-snoRNAs are actively exported to the cytoplasm by the NXF1/NXT1 export machinery. We also noted that the export impairment was accompanied by increased accumulation of mature snoRA75 in the nucleus (Fig. 6*D*). These results were highly reproducible. That is, the export of slb-snoRNAs to the cytoplasm appears to compete with snoRNA maturation.

Finally, we tested if cytoplasmic slb-snoRNAs were also associated with the canonical snoRNA binding proteins. We analyzed cytoplasmic RNA coprecipitated with HA-tagged dyskerin. Both ectopic *xt*slb-snoRA75 and endogenous *xl*slb-snoRA75 were detected in the cytoplasmic RNA coimmunoprecipitated with dyskerin (Fig. 6*C*). The most plausible interpretation of these results is that slb-snoRNAs accumulate in the cytoplasm as RNP particles that still contain dyskerin.

Discussion

SnoRNAs are among the most thoroughly studied noncoding RNAs, yet many questions remain about their biogenesis and functions. The conventional model of snoRNA expression is that they are processed from excised and linearized introns of Pol II transcribed genes. Yet, the expression levels of many intronic snoRNAs cannot be explained by the expression levels of their host genes. Two mechanisms have been proposed to explain the uncoupling of host gene and snoRNA expression levels: nonsense-mediated decay (22) and dual-initiation transcription (23). However, not all snoRNAs and host genes fit these models (24). We found that a subset of snoRNAs, the slb-snoRNAs, become stabilized as lariats. The accumulation of snoRNAs in this form and their further active export to the cytoplasm prevent their processing into mature snoRNA molecules. This accumulation of slb-snoRNAs occurs both tissue-specifically (Figs. 1*C* and 4*D*) and species-specifically (Dataset S1). These findings reveal a pathway for fine regulation of snoRNA expression in the cell.

Compound ncRNAs that contain snoRNAs have been previously described (25–27). However, in the previous cases snoRNA domains were found at the ends of linear RNA molecules; stabilization and protection of the ends are their main function (26–28). In the slb-snoRNAs, the lariat structure itself provides snoRNA sequences with additional protection against exonuclease activities. Importantly, this structure also prevents snoRNAs from functioning as guide RNAs for posttranscriptional modification of rRNAs and snRNAs (Figs. 3–5), even though snoRNAs in the lariat form are associated with core snoRNP proteins, including the modification enzyme dyskerin (Fig. 6). Such exclusion from a pool of functional modification guide RNPs may play a role in negative regulation of posttranscriptional modification of functionally critical cellular RNA. Recent studies identified fractionally modified positions in rRNAs (29–32) and snRNAs (33); these diversified modification patterns generate ribosome and spliceosome heterogeneity. In fact, slb-snoRD RNAs that we identified in HeLa cells (Dataset S1) target either very vulnerable and undermethylated positions in rRNAs, or they modify positions in close proximity to such highly sensitive residues identified in humans (34). These correlations support the proposed regulatory role of slb-snoRNAs.

The inability of slb-snoRNAs to mediate posttranscriptional modifications assigned to their cognate snoRNAs is critical for their proposed regulatory function. Our experiments clearly demonstrate that slb-snoRNAs are not functional modification guide RNAs (Figs. 3–5), which is contrary to the earlier study of endogenous yeast snoRNA function in the *dbr1Δ* strain (4). These discrepancies can be easily explained by the presence of partially processed snoRNAs in the mutant yeasts; particularly, box C/D snoRNAs were found functional even when they were not fully processed.

One could argue that slb-snoRNAs show no modification activities because lariats are rapidly exported to the cytoplasm, and therefore they become separated from their substrate in the nucleus. Indeed, an excess of lariats in the nucleus is toxic for cells, and their export to the cytoplasm was demonstrated in yeast cells deficient for DBR1 (35). However, in *Xenopus* GVs some slb-snoRNAs accumulate at levels comparable to that of fully processed snoRNAs (Figs. 1*C* and 4*D*). Specifically, *X. laevis* slb-snoRA75 is one such example, yet *X. laevis* snoRA75 in the lariat form does not support modification of 18S rRNA (Fig. 4*E*).

Intriguingly, the circularization of a snoRNA does not alone eliminate its ability to mediate posttranscriptional modification. Archaeal circular snoRNA-like RNAs are fully functional modification guide RNAs (36–38). These circular guide RNAs belong to a class of stable circular RNAs called tRNA intronic circular (tric)RNA (39). Why are tricRNAs functional modification guide RNAs but not slb-snoRNAs? It is possible that slb-snoRNAs are too bulky relative to mature snoRNAs and tricRNAs. Archaeal circular guides have only 2 to 3 extra nucleotides, whereas slb-snoRNAs are at least 100 nt longer than mature snoRNAs. Such additional sequence might affect overall snoRNA folding or stabilize nonfunctional alternative

conformations. Although no dramatic changes were predicted in snoRNA domains of most slb-snoRNAs using RNA folding software algorithms (*SI Appendix*, Fig. S6), even minor alterations in snoRNA structure can turn fully functional modification guide RNPs into nonfunctional (20). Additionally, slb-snoRNAs have a 5′–2′ covalent bond linking the branchpoint to the 5′ end of the intron, whereas tricRNAs consist of regular 5′–3′ links throughout.

We should emphasize here that snoRNA functions are not limited to canonical guide RNA activities and rRNA processing (40–44). Dysregulation of snoRNAs is associated with many diseases, and some snoRNAs have been proposed to have oncogenic or tumor-suppressive functions (45–49). In some cases, the link between a single snoRNA and tumor progression involves misregulation of modifications in rRNA (50) or spliceosomal snRNA (51), although these are rather rare examples. The underlying mechanism could be associated with smaller RNAs processed from snoRNAs. These include microRNAs (miRNAs), PIWI interacting RNAs, and snoRNA-derived RNAs (sdRNAs), which regulate transcription, translation, and alternative splicing (52–58). Thus, the stabilization of sdRNA precursors as slb-snoRNAs would affect processing and function of both snoRNAs and sdRNAs. Intriguingly, among the human slb-snoRNAs that we report here (Dataset S1), four contain snoRNAs up-regulated in cancers: U27, U64, U38B, and U105B.

Different conditions, stress factors, and drugs can change snoRNA expression and cellular distribution (59–64). In response to lipotoxic and oxidative stress, some snoRNAs accumulate in the cytoplasm (61, 63). The export mechanism requires further study (65). It is possible that these snoRNAs are exported in the form of slb-snoRNAs and, under stress conditions, become further processed to the mature form in the cytoplasm. Consistent with this hypothesis, DBR1 has been shown to shuttle between the nucleus and the cytoplasm (66).

Furthermore, slb-snoRNAs may regulate the availability of RNA binding proteins in the cell. It has been shown that artificial accumulation of lariats, driven by knockdown of the debranching enzyme, led to sequestration of the RNA-binding protein TDP-43 in yeast and mammalian cells (35). It is known that TDP-43 binds transiently to introns and regulates many cellular processes. In plants, Dicer, an endonuclease required for miRNA processing, can be sequestered in a similar manner, resulting in a general down-regulation of miRNAs (15). It is possible that slb-snoRNAs are necessary to sequester snoRNA binding proteins. In fact, many stable lariats contain snoRNA-like motifs (e.g., human slb-snoRA29) (Dataset S1) rather than typical snoRNAs; the latter form fully processed functional snoRNPs. Because dysregulation of snoRNA binding proteins is prominent in some diseases (67–70), their tight regulation is essential.

Concluding Remarks

In this study we reported hundreds of snoRNAs that normally accumulate in the form of stable lariats instead of fully processed snoRNP particles. This type of ncRNA is wide-spread across different species. We proposed that the main function for this unusual form of snoRNA is the fine-tuning of expression levels of mature snoRNAs and modification guide snoRNPs. Since more than 15% of snoRNAs show some level of tissue specificity (24), and little overlap of slb-snoRNAs was found between different species (our data), we predict that more slb-snoRNAs will be identified when more species and cell types are analyzed. As ever more diversified functions of snoRNAs themselves are discovered, we predict that the roles of slb-snoRNAs will also expand beyond the regulation of snoRNA expression.

Materials and Methods

Cell Culture and Transfection. Human HeLa and mouse 3T3 cell lines were cultured according to standard procedures. HeLa cells were transfected using ViaFect reagent (Promega). SnoRA29 expression constructs are depicted in Fig. 3*C*. Fragments of snoRNA-coding genes were amplified from genomic DNAs and cloned into the pCS2 vector under the CMV promoter.

Animals, Oocytes, and Microinjections. *X. laevis* females were anesthetized with tricaine methanesulfonate (MS222), pH 7.0, and a portion of their ovary was removed. Manually separated oocytes were injected at the animal pole with 100 pg of plasmid in a 2.3-nL volume, unless otherwise stated. After injection, oocytes were incubated in OR2 for 2 d. Oocytes were dissected in a pH 5.6 isolation solution (83 mM KCl, 17 mM NaCl, 6.0 mM Na_2HPO_4, 4.0 mM KH_2PO4, 1 mM $MgCl_2$, 1.0 mM DTT) to separate nuclear and cytoplasmic fractions.

Human dyskerin cDNA was amplified from a construct provided by Mary Armanios, The Johns Hopkins University School of Medicine, Baltimore, MD, and a C-terminal HA-tag was added with a reverse primer. The PCR fragment was cloned into pcDNA3 vector under the CMV promoter. A construct to express *xt*slb-snora75 was generated as previously described (10).

Yeast Strains and Plasmids. Haploid yeast *Saccharomyces cerevisiae* strains used in this study were the following: BY4741 (a wild-type control), the *dbr1Δ, DBR1::KAN* mutant strain (kindly provided by Jeff Han, Tulane University School of Medicine, New Orleans, LA), and the double-knockout *dbr1Δrnt1Δ, DBR1::HIS RNT1::TRP* strain (kindly provided by Sherif Abou Elela, Université de Sherbrooke, Sherbrooke, QC, Canada).

To express exogenous RNAs in yeast cells, corresponding coding sequences were amplified from genomic DNAs and cloned into p426Gal1 and p416GalS vectors and into the YEplac195 plasmid containing a *GPD* promoter, an RNT1 cleavage site, and an *snR13* terminator (71). The RNT1 cleavage site was removed from the constructs that were expressed in *dbr1Δrnt1Δ* strain. Overlap-extension PCR was used to make chimeric fragments. Schematic representation of these constructs is shown in Fig. 5*A*. Yeast cells were transformed using standard lithium acetate methods. At least two to three independent colonies were analyzed from each plate. Transformants were grown in SC-URA medium with either glucose or galactose as a source of sugar at 30 °C, or at 25 °C when the *dbr1Δrnt1Δ* mutant strain was used in the experimental set-up.

RNA Purification. TRIzol reagent (Ambion) was used to extract RNA from vertebrate cell lines and *Xenopus* oocytes. Hot acid phenol was used for yeast RNA extraction. RNA was purified using the Direct-zol RNA MiniPrep kit (Zymo Research). DNA was removed on the columns according to the manufacturer's protocol.

RNA Coimmunoprecipitation. Oocytes were dissected in isolation buffer adjusted to pH 7.0. Nuclear and cytoplasmic fractions were collected in separate tubes and homogenized in a lysis buffer (20 mM TrisHCl, pH 7.4, 150 mM NaCl, 5 mM $MgCl_2$, 1 mM DTT) with a proteinase inhibitor mixture (Roche). The lysates were incubated with anti-HA magnetic beads (Pierce) for 1 h at room temperature. Coprecipitated RNA was extracted with TRIzol.

Northern Blotting. RNA was separated on an 8% urea polyacrylamide gel, transferred onto a nylon membrane (Zeta Probe, Bio-Rad), and probed with digoxigenin (Dig)-labeled DNA probes, specific for yeast and vertebrate snoRNAs. Dig was detected with an anti-Dig antibody conjugated with alkaline phosphatase and the chemiluminescent substrate CDP-Star (Roche). Hybridization signals were visualized and analyzed using a Li-Cor Odyssey Fc imaging system and Image Studio software. All Northern blots were repeated twice.

RT-PCR Analysis. Reverse transcription was performed using random hexamers with Episcript-RT (Epicentre) and AMV-RT (New England Biolabs) for 1 h at 37 °C. cDNA was amplified with inward and outward facing primers (*SI Appendix*, Table S1) using Taq DNA polymerase. RT-PCR experiments were performed in two independent replicates. To confirm the specificity of the amplified sequences, PCR fragments were cloned into the pGEM-T Easy vector (Promega) and sequenced.

Fluorescent Primer Extension Analysis of Posttranscriptional Modifications. For mapping 2′-*O*-methylated and pseudouridylated residues in yeast and vertebrate RNAs, we used nonradioactive modifications of reverse transcription-based methods described in Deryusheva and Gall (72). The 6-FAM–labeled oligonucleotides specific for yeast U2 snRNA and rRNAs were previously designed (7, 73). In brief, to detect 2′-*O*-methylation, we performed primer

extension with a low concentration of dNTP (0.004 mM). To detect pseudouridines, RNA samples were treated first with CMC [*N*-cyclohexyl-N′-(2-morpholinoethyl) carbodiimide metho-p-toluene sulfonate] (Sigma-Aldrich) and then with 50 mM sodium carbonate buffer (pH 10.4). Fragments were separated on a capillary electrophoresis instrument (Applied Biosystems) using techniques and parameters suggested by the manufacturer. The Gene Scan-500 Liz Size Standard was included in each run to align fragments from different samples. GeneMapper software (Applied Biosystems) was used to screen the data, identify peaks, and precisely map modified nucleotides. All RNA modification analysis experiments were done in duplicates; each sample was run on capillary columns in three serial dilutions.

Bioinformatics. The datasets used in this study have been deposited in the National Center for Biotechnology Information (NCBI) Sequence Read Archive (SRA) BioProject IDs PRJNA302326 and PRJNA479418. Stable lariats were previously annotated (10, 18). In short, conventional reads were aligned with TopHat (v2.0.7) to the *X. tropicalis* genome (v9.1), the mouse genome (v10), the human genome (v19), the chicken genome (v5), or the *X. laevis* genome (v9.0), and intronic reads were quantified with Bedtools (v2.15.0). To further verify the circular nature of lariats, inverted reads were mapped using find_lariat.pl (74). SnoRNA-like motifs were identified with snoReport (v2) (19).

Data Availability. RNA sequencing data used in this study are available at https://www.ncbi.nlm.nih.gov/bioproject/PRJNA302326/ (18) and https://www.ncbi.nlm.nih.gov/bioproject/PRJNA479418/ (10). All other data are included in the main text and supporting information.

ACKNOWLEDGMENTS. Research reported in this publication was supported by the National Institute of General Medical Sciences of the NIH under award R01 GM33397 (to J.G.G.). J.G.G. is American Cancer Society Professor of Developmental Genetics.

1. Y.-T. Yu, R. M. Terns, M. P. Terns, "Mechanisms and functions of RNA-guided RNA modification" in *Fine-Tuning of RNA Functions by Modification and Editing*, H. Grosjean, Ed. (Springer Berlin Heidelberg, 2005), pp. 223–262.
2. P. Vitali, T. Kiss, Cooperative 2′-O-methylation of the wobble cytidine of human elongator tRNA^{Met}(CAT) by a nucleolar and a Cajal body-specific box C/D RNP. *Genes Dev.* **33**, 741–746 (2019).
3. K. B. Chapman, J. D. Boeke, Isolation and characterization of the gene encoding yeast debranching enzyme. *Cell* **65**, 483–492 (1991).
4. S. L. Ooi, D. A. Samarsky, M. J. Fournier, J. D. Boeke, Intronic snoRNA biosynthesis in Saccharomyces cerevisiae depends on the lariat-debranching enzyme: Intron length effects and activity of a precursor snoRNA. *RNA* **4**, 1096–1110 (1998).
5. E. Petfalski, T. Dandekar, Y. Henry, D. Tollervey, Processing of the precursors to small nucleolar RNAs and rRNAs requires common components. *Mol. Cell. Biol.* **18**, 1181–1189 (1998).
6. G. Chanfreau, G. Rotondo, P. Legrain, A. Jacquier, Processing of a dicistronic small nucleolar RNA precursor by the RNA endonuclease Rnt1. *EMBO J.* **17**, 3726–3737 (1998).
7. S. Deryusheva, G. J. S. Talhouarne, J. G. Gall, "Lost and found": snoRNA Annotation in the Xenopus genome and implications for evolutionary studies. *Mol. Biol. Evol.* **37**, 149–166 (2020).
8. E. J. Gardner, Z. F. Nizami, C. C. Talbot Jr, J. G. Gall, Stable intronic sequence RNA (sisRNA), a new class of noncoding RNA from the oocyte nucleus of Xenopus tropicalis. *Genes Dev.* **26**, 2550–2559 (2012).
9. Y. Zhang *et al.*, Circular intronic long noncoding RNAs. *Mol. Cell* **51**, 792–806 (2013).
10. G. J. S. Talhouarne, J. G. Gall, Lariat intronic RNAs in the cytoplasm of vertebrate cells. *Proc. Natl. Acad. Sci. U.S.A.* **115**, E7970–E7977 (2018).
11. A. Jacquier, M. Rosbash, RNA splicing and intron turnover are greatly diminished by a mutant yeast branch point. *Proc. Natl. Acad. Sci. U.S.A.* **83**, 5835–5839 (1986).
12. J. W. Pek, I. Osman, M. L. Tay, R. T. Zheng, Stable intronic sequence RNAs have possible regulatory roles in Drosophila melanogaster. *J. Cell Biol.* **211**, 243–251 (2015).
13. M. L. Tay, J. W. Pek, Maternally inherited stable intronic sequence RNA triggers a self-reinforcing feedback loop during development. *Curr. Biol.* **27**, 1062–1067 (2017).
14. L. Stoll *et al.*, A circular RNA generated from an intron of the insulin gene controls insulin secretion. *Nat. Commun.* **11**, 5611 (2020).
15. Z. Li *et al.*, Intron lariat RNA inhibits MicroRNA biogenesis by sequestering the dicing complex in arabidopsis. *PLoS Genet.* **12**, e1006422 (2016).
16. W. N. Moss, J. A. Steitz, Genome-wide analyses of Epstein-Barr virus reveal conserved RNA structures and a novel stable intronic sequence RNA. *BMC Genomics* **14**, 543 (2013).
17. V. S. Tompkins, D. P. Valverde, W. N. Moss, Human regulatory proteins associate with non-coding RNAs from the EBV IR1 region. *BMC Res. Notes* **11**, 139 (2018).
18. G. J. Talhouarne, J. G. Gall, Lariat intronic RNAs in the cytoplasm of Xenopus tropicalis oocytes. *RNA* **20**, 1476–1487 (2014).
19. J. V. de Araujo Oliveira *et al.*, SnoReport 2.0: New features and a refined support vector machine to improve snoRNA identification. *BMC Bioinformatics* **17**(suppl. 18), 464 (2016).
20. S. Deryusheva, J. G. Gall, Orchestrated positioning of post-transcriptional modifications at the branch point recognition region of U2 snRNA. *RNA* **24**, 30–42 (2018).
21. A. M. Kiss, B. E. Jády, E. Bertrand, T. Kiss, Human box H/ACA pseudouridylation guide RNA machinery. *Mol. Cell. Biol.* **24**, 5797–5807 (2004).
22. S. Lykke-Andersen *et al.*, Human nonsense-mediated RNA decay initiates widely by endonucleolysis and targets snoRNA host genes. *Genes Dev.* **28**, 2498–2517 (2014).
23. C. Nepal *et al.*, Dual-initiation promoters with intertwined canonical and TCT/TOP transcription start sites diversify transcript processing. *Nat. Commun.* **11**, 168 (2020).
24. É. Fafard-Couture, D. Bergeron, S. Couture, S. Abou-Elela, M. S. Scott, Annotation of snoRNA abundance across human tissues reveals complex snoRNA-host gene relationships. *Genome Biol.* **22**, 172 (2021).
25. J. R. Mitchell, J. Cheng, K. Collins, A box H/ACA small nucleolar RNA-like domain at the human telomerase RNA 3′ end. *Mol. Cell. Biol.* **19**, 567–576 (1999).
26. Q. F. Yin *et al.*, Long noncoding RNAs with snoRNA ends. *Mol. Cell* **48**, 219–230 (2012).
27. H. Wu *et al.*, Unusual processing generates SPA LncRNAs that sequester multiple RNA binding proteins. *Mol. Cell* **64**, 534–548 (2016).
28. E. H. Blackburn, K. Collins, Telomerase: An RNP enzyme synthesizes DNA. *Cold Spring Harb. Perspect. Biol.* **3**, a003558 (2011).
29. N. Krogh *et al.*, Profiling of 2′-O-Me in human rRNA reveals a subset of fractionally modified positions and provides evidence for ribosome heterogeneity. *Nucleic Acids Res.* **44**, 7884–7895 (2016).
30. M. Taoka *et al.*, The complete chemical structure of Saccharomyces cerevisiae rRNA: Partial pseudouridylation of U2345 in 25S rRNA by snoRNA snR9. *Nucleic Acids Res.* **44**, 8951–8961 (2016).
31. M. Taoka *et al.*, Landscape of the complete RNA chemical modifications in the human 80S ribosome. *Nucleic Acids Res.* **46**, 9289–9298 (2018).
32. S. Sharma, V. Marchand, Y. Motorin, D. L. J. Lafontaine, Identification of sites of 2′-O-methylation vulnerability in human ribosomal RNAs by systematic mapping. *Sci. Rep.* **7**, 11490 (2017).
33. N. Krogh, M. Kongsbak-Wismann, C. Geisler, H. Nielsen, Substoichiometric ribose methylations in spliceosomal snRNAs. *Org. Biomol. Chem.* **15**, 8872–8876 (2017).
34. J. Bizarro *et al.*, Nopp140-chaperoned 2′-O-methylation of small nuclear RNAs in Cajal bodies ensures splicing fidelity. *Genes Dev.* **35**, 1123–1141 (2021).
35. M. Armakola *et al.*, Inhibition of RNA lariat debranching enzyme suppresses TDP-43 toxicity in ALS disease models. *Nat. Genet.* **44**, 1302–1309 (2012).
36. S. R. Salgia, S. K. Singh, P. Gurha, R. Gupta, Two reactions of Haloferax volcanii RNA splicing enzymes: Joining of exons and circularization of introns. *RNA* **9**, 319–330 (2003).
37. N. G. Starostina *et al.*, Circular box C/D RNAs in Pyrococcus furiosus. *Proc. Natl. Acad. Sci. U.S.A.* **101**, 14097–14101 (2004).
38. M. Danan, S. Schwartz, S. Edelheit, R. Sorek, Transcriptome-wide discovery of circular RNAs in Archaea. *Nucleic Acids Res.* **40**, 3131–3142 (2012).
39. Z. Lu *et al.*, Metazoan tRNA introns generate stable circular RNAs in vivo. *RNA* **21**, 1554–1565 (2015).
40. O. A. Youssef *et al.*, Potential role for snoRNAs in PKR activation during metabolic stress. *Proc. Natl. Acad. Sci. U.S.A.* **112**, 5023–5028 (2015).
41. M. Falaleeva *et al.*, Dual function of C/D box small nucleolar RNAs in rRNA modification and alternative pre-mRNA splicing. *Proc. Natl. Acad. Sci. U.S.A.* **113**, E1625–E1634 (2016).
42. K. A. Brandis *et al.*, Box C/D small nucleolar RNA (snoRNA) U60 regulates intracellular cholesterol trafficking. *J. Biol. Chem.* **288**, 35703–35713 (2013).
43. M. Falaleeva, J. R. Welden, M. J. Duncan, S. Stamm, C/D-box snoRNAs form methylating and non-methylating ribonucleoprotein complexes: Old dogs show new tricks. *BioEssays* **39**, 10.1002/bies.201600264 (2017).
44. D. Bergeron, É. Fafard-Couture, M. S. Scott, Small nucleolar RNAs: Continuing identification of novel members and increasing diversity of their molecular mechanisms of action. *Biochem. Soc. Trans.* **48**, 645–656 (2020).
45. J. Liao *et al.*, Small nucleolar RNA signatures as biomarkers for non-small-cell lung cancer. *Mol. Cancer* **9**, 198 (2010).
46. L. S. Chang, S. Y. Lin, A. S. Lieu, T. L. Wu, Differential expression of human 5S snoRNA genes. *Biochem. Biophys. Res. Commun.* **299**, 196–200 (2002).
47. X. Fang *et al.*, SNORD126 promotes HCC and CRC cell growth by activating the PI3K-AKT pathway through FGFR2. *J. Mol. Cell Biol.* **9**, 243–255 (2017).
48. Z. Siprashvili *et al.*, The noncoding RNAs SNORD50A and SNORD50B bind K-Ras and are recurrently deleted in human cancer. *Nat. Genet.* **48**, 53–58 (2016).
49. M. Deogharia, M. Majumder, Guide snoRNAs: Drivers or passengers in human disease? *Biology* **8**, 1 (2018).
50. M. McMahon *et al.*, A single H/ACA small nucleolar RNA mediates tumor suppression downstream of oncogenic RAS. *eLife* **8**, e48847 (2019).
51. G. Beneventi, *et al.*, The small Cajal body-specific RNA 15 (SCARNA15) directs p53 and redox homeostasis via selective splicing in cancer cells. *NAR Cancer* **3**, zcab026 (2021).
52. C. Ender *et al.*, A human snoRNA with microRNA-like functions. *Mol. Cell* **32**, 519–528 (2008).
53. R. J. Taft *et al.*, Small RNAs derived from snoRNAs. *RNA* **15**, 1233–1240 (2009).
54. S. Kishore *et al.*, The snoRNA MBII-52 (SNORD 115) is processed into smaller RNAs and regulates alternative splicing. *Hum. Mol. Genet.* **19**, 1153–1164 (2010).

55. M. Brameier, A. Herwig, R. Reinhardt, L. Walter, J. Gruber, Human box C/D snoRNAs with miRNA like functions: Expanding the range of regulatory RNAs. *Nucleic Acids Res.* **39**, 675–686 (2011).
56. M. S. Scott *et al.*, Human box C/D snoRNA processing conservation across multiple cell types. *Nucleic Acids Res.* **40**, 3676–3688 (2012).
57. X. He *et al.*, An Lnc RNA (GAS5)/SnoRNA-derived piRNA induces activation of TRAIL gene by site-specifically recruiting MLL/COMPASS-like complexes. *Nucleic Acids Res.* **43**, 3712–3725 (2015).
58. A. M. Mleczko *et al.*, Levels of sdRNAs in cytoplasm and their association with ribosomes are dependent upon stress conditions but independent from snoRNA expression. *Sci. Rep.* **9**, 18397 (2019).
59. M. S. Chen, P. C. Goswami, A. Laszlo, Differential accumulation of U14 snoRNA and hsc70 mRNA in Chinese hamster cells after exposure to various stress conditions. *Cell Stress Chaperones* **7**, 65–72 (2002).
60. B. Rogelj, C. E. Hartmann, C. H. Yeo, S. P. Hunt, K. P. Giese, Contextual fear conditioning regulates the expression of brain-specific small nucleolar RNAs in hippocampus. *Eur. J. Neurosci.* **18**, 3089–3096 (2003).
61. C. I. Michel *et al.*, Small nucleolar RNAs U32a, U33, and U35a are critical mediators of metabolic stress. *Cell Metab.* **14**, 33–44 (2011).
62. B. I. Laufer *et al.*, Long-lasting alterations to DNA methylation and ncRNAs could underlie the effects of fetal alcohol exposure in mice. *Dis. Model. Mech.* **6**, 977–992 (2013).
63. C. L. Holley *et al.*, Cytosolic accumulation of small nucleolar RNAs (snoRNAs) is dynamically regulated by NADPH oxidase. *J. Biol. Chem.* **290**, 11741–11748 (2015).
64. J. M. Rimer *et al.*, Long-range function of secreted small nucleolar RNAs that direct 2′-*O*-methylation. *J. Biol. Chem.* **293**, 13284–13296 (2018).
65. M. W. Li *et al.*, Nuclear export factor 3 regulates localization of small nucleolar RNAs. *J. Biol. Chem.* **292**, 20228–20239 (2017).
66. N. Kataoka, I. Dobashi, M. Hagiwara, M. Ohno, hDbr1 is a nucleocytoplasmic shuttling protein with a protein phosphatase-like motif essential for debranching activity. *Sci. Rep.* **3**, 1090 (2013).
67. T. Sbarrato *et al.*, A ribosome-related signature in peripheral blood CLL B cells is linked to reduced survival following treatment. *Cell Death Dis.* **7**, e2249 (2016).
68. B. Han *et al.*, Human DBR1 modulates the recycling of snRNPs to affect alternative RNA splicing and contributes to the suppression of cancer development. *Oncogene* **36**, 5382–5391 (2017).
69. S. Lykke-Andersen, B. K. Ardal, A. K. Hollensen, C. K. Damgaard, T. H. Jensen, Box C/D snoRNP autoregulation by a *cis*-acting snoRNA in the NOP56 Pre-mRNA. *Mol. Cell* **72**, 99–111.e5 (2018).
70. J. Zhang, G. Yang, Q. Li, F. Xie, Increased fibrillarin expression is associated with tumor progression and an unfavorable prognosis in hepatocellular carcinoma. *Oncol. Lett.* **21**, 92 (2021).
71. C. Huang, J. Karijolich, Y. T. Yu, Post-transcriptional modification of RNAs by artificial Box H/ACA and Box C/D RNPs. *Methods Mol. Biol.* **718**, 227–244 (2011).
72. S. Deryusheva, J. G. Gall, Small Cajal body-specific RNAs of Drosophila function in the absence of Cajal bodies. *Mol. Biol. Cell* **20**, 5250–5259 (2009).
73. S. Deryusheva, J. G. Gall, Novel small Cajal-body-specific RNAs identified in Drosophila: Probing guide RNA function. *RNA* **19**, 1802–1814 (2013).
74. A. J. Taggart *et al.*, Large-scale analysis of branchpoint usage across species and cell lines. *Genome Res.* **27**, 639–649 (2017).